

1 Conformational Heterogeneity of Unbound Proteins Enhances 2 Recognition in Protein–Protein Encounters

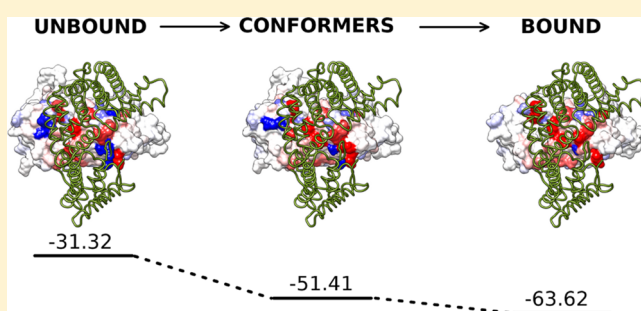
3 Chiara Pallara,[†] Manuel Rueda,[‡] Ruben Abagyan,[‡] and Juan Fernández-Recio^{*,†}

4 [†]Joint BSC-CRG-IRB Research Program in Computational Biology, Life Sciences Department, Barcelona Supercomputing Center,
5 C/Jordi Girona 29, Barcelona 08034, Spain

6 [‡]Skaggs School of Pharmacy and Pharmaceutical Sciences, University of California, San Diego, 9500 Gilman Drive, La Jolla, California
7 92093, United States

8 **S** Supporting Information

9 **ABSTRACT:** To understand cellular processes at the
10 molecular level we need to improve our knowledge of
11 protein–protein interactions, from a structural, mechanistic,
12 and energetic point of view. Current theoretical studies and
13 computational docking simulations show that protein dynam-
14 ics plays a key role in protein association and support the need
15 for including protein flexibility in modeling protein inter-
16 actions. Assuming the conformational selection binding
17 mechanism, in which the unbound state can sample bound
18 conformers, one possible strategy to include flexibility in
19 docking predictions would be the use of conformational
20 ensembles originated from unbound protein structures. Here we present an exhaustive computational study about the use of
21 precomputed unbound ensembles in the context of protein docking, performed on a set of 124 cases of the Protein–Protein
22 Docking Benchmark 3.0. Conformational ensembles were generated by conformational optimization and refinement with
23 MODELER and by short molecular dynamics trajectories with AMBER. We identified those conformers providing optimal
24 binding and investigated the role of protein conformational heterogeneity in protein–protein recognition. Our results show that
25 a restricted conformational refinement can generate conformers with better binding properties and improve docking encounters
26 in medium-flexible cases. For more flexible cases, a more extended conformational sampling based on Normal Mode Analysis
27 was proven helpful. We found that successful conformers provide better energetic complementarity to the docking partners, which is
28 compatible with recent views of binding association. In addition to the mechanistic considerations, these findings could be
29 exploited for practical docking predictions of improved efficiency.



30 ■ INTRODUCTION

31 Proteins are key components in the cell and function through
32 intricate networks of interactions¹ that are involved in virtually
33 all relevant biological processes, such as gene expression and
34 regulation, enzyme catalysis, immune response, or signal
35 transduction.^{2,3} Understanding such interactions at the
36 molecular level is essential to target them for therapeutic or
37 biotechnological purposes. X-ray crystallography and NMR
38 techniques have produced a wealth of structural data on
39 protein–protein complexes, which has largely extended our
40 knowledge on molecular recognition and protein association
41 mechanism and has fostered drug discovery. However, such
42 structural data covers only a tiny fraction of the estimated
43 number of protein–protein complexes formed in cell,⁴ and,
44 therefore, computational approaches that can complement such
45 experimental efforts are strongly needed. In recent years, a
46 variety of protein–protein docking methods have been
47 reported, based either on template modeling^{5–7} or on *ab initio*
48 algorithms. Geometry-based methods try to find the best
49 surface complementarity between interacting proteins, using
50 simplified structural models and approximate scoring functions.

51 A popular strategy is to discretize the proteins into grids and
52 use Fast Fourier Transform (FFT) algorithms⁸ to accelerate
53 search on the translational space, such as in FTDock,⁹ PIPER,¹⁰
54 GRAMM-X,¹¹ ZDOCK,¹² or on the rotational space, as in
55 Hex¹³ or FRODOCK.¹⁴ Another strategy to explore surface
56 complementarity is geometric hashing, as used in PatchDock.¹⁵
57 Docking methods based on energy optimization use a variety of
58 sampling strategies based on molecular mechanics, such as
59 molecular dynamics in HADDOCK,¹⁶ or Monte Carlo
60 minimization in RosettaDock¹⁷ or ICM-DISCO.¹⁸ The
61 function used to identify the best orientations is an important
62 aspect of docking, and dedicated scoring schemes have been
63 developed, based on energy terms, such as in pyDock,¹⁹ or on
64 statistical potentials as in SIPPER²⁰ or PIE.²¹ The Critical
65 Assessment of PRediction of Interactions (CAPRI; <http://www.ebi.ac.uk/msd-srv/capri/>)
66 experiment has indeed shown
67 that accurate models can be produced by docking in many of

Received: February 25, 2016

68 the cases.²² However, there are other cases in which all docking
69 methods systematically fail, typically the most flexible ones.^{23,24}
70 Thus, one of the major challenges in docking is how to deal
71 with molecular flexibility and conformational changes that
72 happen upon association.^{23,24} A major hurdle is the computa-
73 tional cost of integrating docking and conformational search,
74 aggravated by our limited knowledge of the protein–protein
75 association mechanism. Different mechanisms for flexible
76 protein–protein binding have been proposed. Perhaps the
77 most widespread view is the induced-fit mechanism, in which
78 the interacting partners are involved in initial encounters that
79 evolve toward the final specific complex by adjusting their
80 interfaces. Most of the reported methods for flexible docking
81 try to mimic this mechanism, typically using an initial rigid-
82 body search followed by a final refinement of the interfaces as
83 in ICM-DISCO,²⁵ HADDOCK,¹⁶ RosettaDock,¹⁷ or Fiber-
84 Dock²⁶ or by integrating small deformations of the global
85 structures during the sampling based on normal modes as in
86 ATTRACT^{27,28} or SwarmDock.²⁹
87 An alternative mechanism is conformational selection, which
88 was initially proposed for systems in which the ligand
89 selectively binds one of the conformers of the dynamically
90 fluctuating receptor protein.^{30,31} This was generalized to the
91 “conformational selection and population shift” concept, which
92 postulated that flexible proteins in solution naturally sample a
93 variety of conformational states, and the ligand protein
94 preferentially binds to a pre-existing subpopulation of such
95 conformers, thus adjusting the equilibrium in favor of
96 them.^{32–34} Recently, the conformational selection model has
97 been extended to include different mutual conformational
98 selection and adjustment steps,³⁵ so that the unbound
99 conformational states that are available for mutual selection
100 might not be initially in the bound conformation. The
101 conformational selection model has been largely supported by
102 several structural studies including MD, NMA, X-ray
103 crystallography, and NMR experiments,^{35–39} and later strongly
104 confirmed by theoretical analysis based on the correlation
105 between complex association/dissociation rates and several
106 molecular descriptors detailing specific features of protein
107 intrinsic flexibility and complex formation.⁴⁰ This mechanism
108 can be implemented in a computational docking strategy by
109 using precomputed ensembles of unbound proteins, which
110 ideally contain conformers that are suitable for binding the
111 interacting partner. However, to date this strategy has not been
112 really used for practical protein–protein docking predictions.
113 Most of the prior studies were limited to the use of a few
114 selected conformers and/or applied to specific cases of
115 interest.^{41–43} Unexpectedly, the few systematic analyses
116 published so far^{44–46} failed to improve the structural prediction
117 of protein complexes with respect to the unbound structure.
118 This could be related to an unrealistic representation of the
119 motions occurring in the time scale of molecular association or
120 to the use of only a few conformers.^{44–46} Indeed, for small
121 proteins like ubiquitin it is possible to obtain more
122 representative ensembles, based on RDC data, which are
123 definitely useful in docking predictions.⁴⁷ However, this
124 approach is difficult to generalize for large scale predictions
125 due to experimental limitations. Therefore, it would be
126 important to find practical ways of generating ensembles that
127 include conformers that improve binding. This could help not
128 only to improve docking predictions but also to advance toward
129 a better understanding of flexible protein–protein association
130 mechanism. With this purpose in mind, here we used three

different computational approaches to represent the conforma-
tional heterogeneity of the unbound proteins and tested them
on a standard protein–protein docking benchmark. Our
analysis clearly shows that a simple molecular mechanics
minimization approach provides sufficient conformational
heterogeneity to improve docking predictions in medium-
flexible cases, which are the most likely to follow the
conformational selection mechanism.

■ METHODS

Generation of Protein Conformational Ensembles. We used three different computational techniques to generate conformational ensembles starting from the unbound protein structures: MODELER minimization (MM), molecular dynamics simulations (MD), and Normal Modes Analysis (NMA).

Conformational search based on the optimization of a molecular probability density function (PDF) was performed with the comparative modeling program MODELER version 9v10,⁴⁸ using as template the unbound X-ray structure of the same protein, and default parameters. Cofactors and small-molecule ligands, if present in the template structure, were taken into account during the modeling procedure. MODELER minimization (MM) is based on an optimization step using the variable target function method (VTFM) with restrained conjugate gradients (CG), followed by a refinement step using short (a few ps) molecular dynamics (MD) and simulated annealing (SA), with CHARMM parameters and distance-dependent dielectric constant.

Conformational search based on Molecular Dynamics (MD) was performed by a 10 ns long explicit solvent unrestrained MD simulation on the unbound structure using the force field AMBER parm99⁴⁹ and the AMBER8 package.⁵⁰ As a first preparation step, all the missing loops in the protein structures were modeled using the MODELER program. The parametrization of each system was performed using AMBER's module LEAP, whereas the cofactor and small-molecule ligand libraries, when needed, were written with the AMBER modules ANTECHAMBER and LEAP. Each system was then minimized, solvated, and equilibrated at similar conditions to those previously described for the MoDEL database,⁵¹ as follows. First, original PDB coordinates were stripped of hydrogen atoms, monovalent ions, and all water molecules. Noncovalent ligands were kept and parametrized with the GAFF force-field using standard procedures,⁵² and missing side-chain atoms and hydrogen atoms were added from AMBER residue libraries using the LEAP AMBER tool. Each system was relaxed by a short restrained energy minimization (20 steps steepest descent, 80 steps conjugate gradient, restraining all the heavy atoms with a 20 kcal/mol Å² to the initial structure) to relieve highly unfavorable sterical clashes. Then each minimized structure was immersed in a periodic truncated octahedron box containing a 12 Å buffer of TIP3P water molecules, and Na⁺ and Cl[−] counterions were added to the solvent bulk to maintain neutrality of the system and reach 50 mM NaCl ionic strength.

Each solvated system underwent a short solvent minimization and five-step equilibration protocol. First, a 500-cycle steepest descent and a 500-cycle conjugate gradient minimization were performed, applying harmonic restraints with a force constant of 50 kcal/(mol·Å²) to all protein atoms in order to minimize the solvent molecules. Then, the five-step equilibration was performed by applying periodic boundary

193 conditions and computing long-range electrostatics by the
194 particle-mesh Ewald method. At each stage, the integration
195 time step was set to 2 fs, the system pressure to 1 atm, and the
196 nonbonding cutoff distance to 12 Å. The five steps are

197 Step 1: A 40 ps MD simulation was run applying harmonic
198 restraints to all the protein atoms with a force constant of 25
199 kcal/(mol·Å²), raising the temperature to 300 K by Langevin
200 dynamics approach with a collision frequency of 1 fs.

201 Step 2: A 20 ps step was performed, setting the temperature
202 to 300 K and reducing system restraints to 10 kcal/(mol·Å²).

203 Step 3: Another 20 ps simulation was run with 10 kcal/(mol·
204 Å²) restraints only to the protein backbone atoms.

205 Step 4: A further 20 ps simulation was performed, decreasing
206 protein backbone restraints to 5 kcal/(mol·Å²).

207 Step 5: A final 100 ps unrestrained MD simulation was run
208 without any restraint.

209 Finally, a 10 ns MD simulation was performed in
210 isothermal–isobaric ensemble, setting pressure to 1 atm and
211 temperature to 300 K. From each MD simulation, two
212 conformational ensembles were created by extracting trajectory
213 snapshots every 10 or 100 ps. Additionally, a random subset of
214 11 benchmark cases (1ACB, 1AY7, 1D6R, 1E6J, 1GCQ, 1IRA,
215 1JMO, 1PXV, 2HRK, 2CFH, 2COL) was selected for longer
216 simulations. Each protein underwent two 100 ns long explicit
217 solvent unrestrained NPT-MD simulations, at the temperatures
218 of 300 and 340 K, respectively, using the same force field as
219 above.

220 Conformational search based on Normal Mode Analysis
221 (NMA) was performed by an in-house protocol on a small
222 subset of the 6 flexible benchmark cases that show strong
223 binding affinity (in which potential errors in the docking
224 scoring function have a minimal impact). NMA is a powerful
225 modeling technique that allows for a fast and accurate
226 description of the intrinsic movements of biomolecules.
227 Modern interpretations of the procedure use the elastic
228 network model (ENM), first described by Tirion as an all-
229 atom version⁵³ and later reformulated as coarse-grained.⁵⁴ In
230 the ENM, the biomolecule is represented as a network of
231 connected atoms, where each node is connected to all the
232 atoms within a cutoff, and the springs represent the interactions
233 between the nodes. Here we used the Anisotropic Network
234 Model⁵⁴ that describes the protein as a C α model, and we
235 assigned the spring constants by a term that assumes an inverse
236 exponential relationship with the distance,⁵⁵ analog to that from
237 Hinsen.⁵⁶ We tried to enhance the conformational space by
238 introducing an iterative exploratory search. The proposed
239 method is called eNMA (enhanced NMA) and creates enriched
240 structurally diverse ensembles. The algorithm works as follows:

241 Step 1: Starting from the unbound C α atoms, we created 100
242 discrete Cartesian conformers from random combinations of
243 displacements along the first 10 normal modes (as described
244 elsewhere).⁵⁷ The average C α displacement with respect to the
245 original structure was set to ~ 1 Å.

246 Step 2: The resulting conformers were then clustered
247 hierarchically via *average linkage* method (as implemented in
248 *ptraj10*)⁵⁰ to obtain 100 diverse conformations.

249 Step 3: Each conformer from the cluster was sent to Step 1,
250 and the whole cycle was started.

251 Step 4: The process was ended up after 10 iterations.

252 In total, around 100,000 intermediate structures were created
253 per protein, but we only kept the ones resulting from the
254 clustering (i.e., 100×10 iterations = 1,000 discrete
255 conformers). The final structures underwent a last optimization

step with MODELER 9.10. All-atom models were rebuilt by 256
adding missing atoms and side-chains and were atomically 257
refined with MODELER (using the original C α model as 258
template) to fix incorrect bond distances.^{48,58} In addition, 100 259
discrete conformers were randomly selected, and for each of 260
them 10 MODELER models were built. The whole procedure 261
took ~ 2 h per protein (ranging from 40 min for 1ACB ligand, 262
with 70 C α atoms, to 5 h for 1IBR ligand, with 440 C α atoms) 263
on 1 core of an Intel Xeon 3.5 GHz CPU (16GB RAM) Linux 264
workstation. Note that our conformational search was 265
unguided, but it could be also guided in future applications 266
(i.e., selecting the combination of models that provides the best 267
score on a given fitness function). 268

Docking Simulations. For all the dockings experiments, 269
the FTDock docking program⁹ was used to generate 10,000 270
rigid-docking poses based on surface complementary and 271
electrostatics at 0.7 Å grid resolution, and then, each docking 272
solution was evaluated by the energy-based pyDock scoring 273
scheme,¹⁹ based on desolvation, electrostatics, and van der 274
Waals energy contributions. All energy values are shown as 275
arbitrary units. Cofactors, small-molecule ligands, and ions were 276
excluded during the sampling and the scoring calculations in 277
docking. 278

Benchmark. In order to validate the approach proposed 279
here, we used the protein–protein docking benchmark 3.0,⁵⁹ 280
comprising a total of 124 test cases in which the structures of 281
both the free components and the complex are known. We 282
have classified these cases according to the conformational 283
variation of the proteins from the unbound to the bound state 284
(based on the RMSD of C α atoms of the interface residues as 285
defined in the mentioned protein–protein benchmark 3.0), 286
which resulted in the following categories: “rigid” (I-RMSD_{C α} < 287
0.5 Å), “low-flexible” (0.5 Å < I-RMSD_{C α} < 1.0 Å), “medium- 288
flexible” (1.0 Å < I-RMSD_{C α} < 2.0 Å), “flexible” (2.0 Å < I- 289
RMSD_{C α} < 3.0 Å), and “highly flexible” (I-RMSD_{C α} > 3.0 Å). 290
The quality of the docking predictions was evaluated according 291
to the ligand protein C α -RMSD with respect to the complex 292
crystal structure (after superimposing the C α atoms of the 293
receptor molecules). A docking experiment was considered 294
successful if a near-native solution (a docking pose with ligand 295
C α -RMSD < 10 Å) was ranked among the top 10 predictions 296
according to the pyDock scoring function. Structural analyses 297
of proteins, including RMSD and clashes calculations, were 298
performed using the ICM program⁶⁰ (www.molsoft.com). 299

300 ■ RESULTS

**Unbound Conformational Ensembles from Molecular 301
Mechanics Contain Conformers with Better Binding 302
Capabilities than the Unbound Structure.** Here we 303
explored in a systematic way whether a minimal description 304
of the conformational heterogeneity of the interacting proteins 305
could significantly improve their binding capabilities. For that 306
purpose, we generated conformational ensembles from the 307
unbound proteins of the complexes in the protein–protein 308
benchmark 3.0.⁵⁹ Ensembles of 100 conformers were initially 309
generated by using two distinct molecular mechanics 310
procedures: a fast restricted conformational optimization, as 311
implemented in MODELER, and a much more computation- 312
ally demanding molecular dynamics method, as implemented in 313
the AMBER package (see *Methods*). *Figure 1* shows examples 314
of the typical conformational heterogeneity (at backbone and 315
side-chain level) generated by MODELER minimization 316
(MM). The deviation of the interface atoms from the initial 317

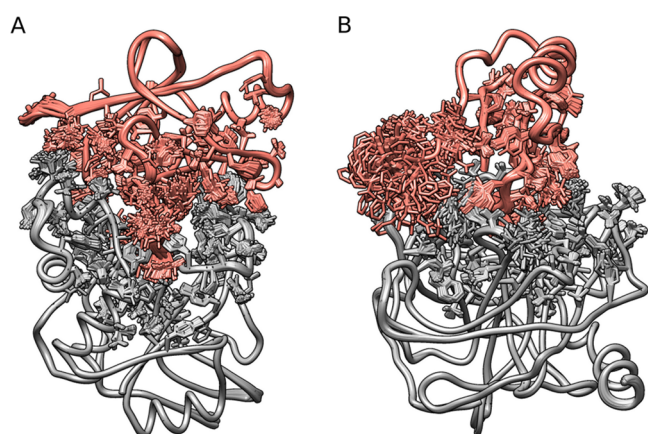


Figure 1. Representative conformational ensembles generated by MODELER minimization. 100 conformers independently generated by MODELER for receptor and ligand proteins are shown for two benchmark cases: (A) 1PXV and (B) 1ACB. Conformers were superimposed onto the corresponding molecules in the reference complexes for visualization. Only interface side chains are shown for the sake of clarity.

318 unbound structure was 1.2 Å RMSD on average (ranging from
319 0.6 Å for the 1R0R receptor to 7.7 Å RMSD for the 2QFW
320 receptor).

321 We compared the unbound models to their corresponding
322 structures in the complex to structurally characterize these
323 conformers and to estimate their capabilities for binding. In
324 order to do that, we first structurally superimposed each model
325 into the corresponding native complex structure (considering
326 only the $C\alpha$ atoms) and then computed the following
327 parameters: (i) the RMSD for all $C\alpha$ atoms ($C\alpha$ -RMSD)
328 with respect to the complex structure; (ii) the RMSD for all
329 interface atoms (Int-RMSD) after superimposing only those
330 interface atoms; (iii) the pyDock binding energy (au) with the
331 bound partner; (iv) the pyDock binding energy (au) with the
332 unbound partner; and (v) the number of clashes with the
333 bound partner. The values for these parameters in the different
334 conformers generated by MODELER are randomly distributed
335 following a Gaussian function (Figure S1). Except for a few
336 cases, such as the viral chemokine binding protein M3 (1ML0
337 receptor), there is no significant correlation between the
338 binding energy of the different conformers in the native
339 orientation and their similarity with respect to the bound
340 structure (Figure 2). Perhaps the main reason for this is that, in
341 general, due to the limited sampling used here, these
342 conformers are not exploring the vicinity of the bound state.
343 Indeed, only 20% of the benchmark proteins contain
344 conformers within 1.0 Å Int-RMSD from the bound state
345 (and in virtually all of these cases the unbound state already had
346 Int-RMSD < 1.0 Å from bound).

347 Ensembles generated by short MD trajectories showed larger
348 conformational variability, but in general they were not closer
349 to the bound state (Figure S1 and S2). Increasing the number
350 of conformers to 1,000 (Figure S3) did not significantly modify
351 the range of conformational variability for either sampling
352 method.

353 We next aimed to identify which conformers of the ensemble
354 seemed more promising for binding. Thus, we selected the best
355 conformers of the ensemble according to the criteria analyzed
356 in the previous paragraphs. Figure 3 shows the best conformers
357 for receptor and ligand proteins identified according to each

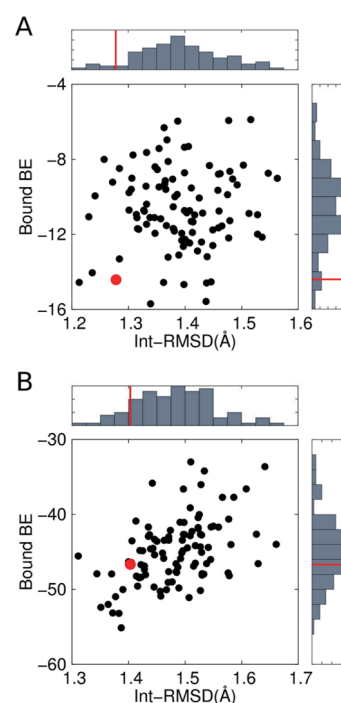


Figure 2. Distribution of geometrical and energetic values for ensemble conformers. The correlation between the full atom interface RMSD (Int-RMSD) with respect to the bound state and the pyDock binding energy (au) toward the bound partner in the native orientation (bound BE) for all conformers in MODELER ensembles are shown for two benchmark cases: (A) 2F0R (1S1Q receptor) and (B) 1MKF (1ML0 receptor). Distribution of Int-RMSD and bound BE values are shown as histograms. Data for the unbound X-ray structure are shown in red.

parameter as compared to the unbound receptor and ligand
structures for all benchmark cases. Regarding the RMSD with
respect to the complex structure, only in a few cases (21% and
6%, according to $C\alpha$ -RMSD and Int-RMSD, respectively) the
best pair of conformers were significantly better (i.e., more than
10% change; averaged for receptor and ligand proteins) than
the unbound X-ray structures. These cases were not particularly
enriched in conformers with Int-RMSD < 1.0 Å. Actually, in
some cases (14% and 36%, according to $C\alpha$ -RMSD and Int-
RMSD, respectively) the best conformers were even farther
from the bound structure than the unbound one.

Interestingly, we found a much higher number of cases in
which the best conformers showed significantly better binding
energy (in 46% and 51% of cases, when considering the bound
or unbound structure as partner, respectively) or fewer clashes
(in 69% of cases) than the unbound X-ray structure. It is
remarkable that the improvement in binding energy was
independent of the structural similarity to the bound structure.
Again, one of the reasons is that in the majority of cases the
limited conformational sampling used here does not permit
reaching the vicinity of the bound state, and, therefore, in such
unbound minima any small improvement toward the bound
state is not relevant in terms of binding energy.

Although MD ensembles showed larger conformational
variability (Figures S1 and S2), the percentage of cases with
conformers that became significantly better than the unbound
state according to each of the above-mentioned criteria (12%,
7%, 37%, 62%, and 69%, respectively) was very similar to those
observed for the MODELER ensembles. However, the 386

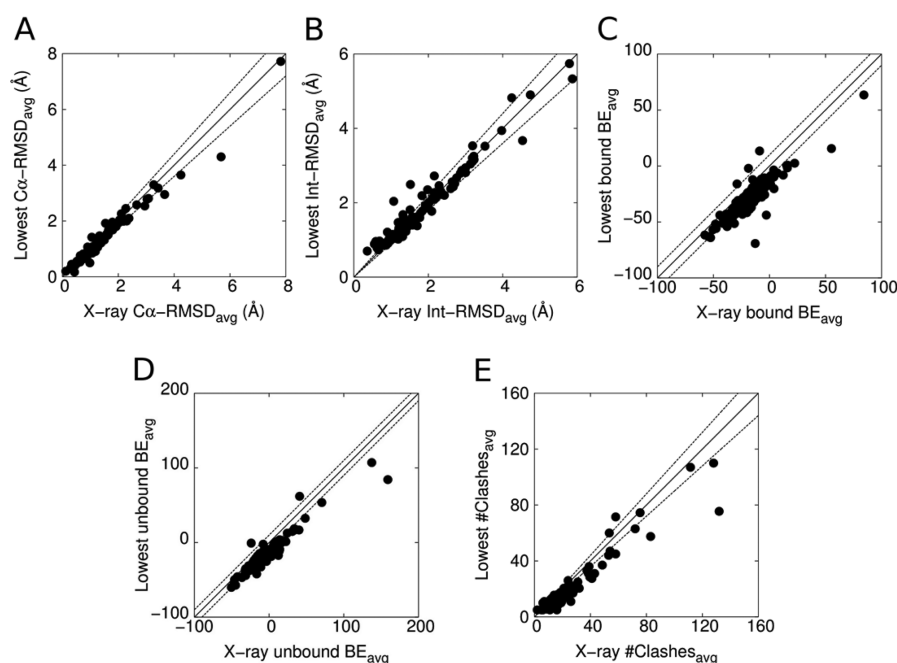


Figure 3. Best ensemble conformers according to quality criteria based on the complex native orientation. For each benchmark case, it is shown the best pairs of receptor and ligand conformers in the conformational ensemble according to the following criteria: (A) $C\alpha$ -RMSD, (B) Int-RMSD, (C) pyDock binding energy with the bound partner (au), (D) pyDock binding energy with the unbound partner (au), (E) number of clashes with respect to the bound partner. The above-described descriptors were calculated independently for the best receptor and ligand conformers and then averaged. These are compared to those of the unbound X-ray structures. Dashed lines represent the (arbitrary) range of variation that we used to consider a change as significant, and it was defined as 10% in the RMSD- and clash-based criteria or 10 au in the energy-based criteria.

387 ensembles generated from the short MD trajectories showed
 388 even more limited conformational sampling in the vicinity of
 389 the bound state, since less than 4% of the benchmark proteins
 390 had conformers with Int-RMSD < 1.0 Å with respect to the
 391 bound state (as compared to 20% in MODELER). Moreover,
 392 in most of the cases (74% and 71%, according to $C\alpha$ -RMSD
 393 and Int-RMSD, respectively) the best conformers from MD
 394 were even farther from the bound structure than the unbound
 395 one. This could be related to the limited sampling of the short
 396 MD simulations used here, as well as to the fact that the protein
 397 structures in solution typically deviates 1–2 Å RMSD from that
 398 in the crystal.⁶¹ Indeed, this is what we observe in our MD
 399 ensembles (Figures S1 and S2). Of course, we should not
 400 disregard possible inaccuracies in the force-field, but they are
 401 usually more relevant in very long trajectories but not so much
 402 in the suboptimal sampling used here.⁶²

403 **Selected Conformers Can Yield Significantly Better**
 404 **Docking Results than Unbound Subunits.** The fact that in
 405 the majority of cases the conformational ensembles contained
 406 conformers that showed better binding energy capabilities than
 407 the unbound X-ray structure encouraged us to evaluate their
 408 use for docking. Since the systematic cross-docking of all
 409 conformers for receptor and ligand proteins would be
 410 impractical, we tried instead to estimate the expected
 411 performance of the unbound ensembles for docking in the
 412 best-case scenario. Therefore, based on the native orientation,
 413 we selected those conformers that seemed the best candidates
 414 to improve the docking predictions according to the criteria
 415 described in the previous section: (i) the lowest $C\alpha$ -RMSD
 416 with respect to the bound state, (ii) the lowest Int-RMSD, (iii)
 417 the best binding energy with the bound partner, (iv) the best
 418 binding energy with the unbound partner, and (v) the smallest
 419 number of clashes with the bound partner. These conformers

were used in protein–protein docking as described in the
 420 **Methods** section. 421

422 **Figure 4A** shows the docking success rates for the top 10
 423 predictions when using these selected conformers, with all the
 424 details in **Table 1**. Interestingly, the results do not significantly
 425 change when using a larger number of conformers (1,000)
 426 generated by MODELER (and applying the same procedure for
 427 selecting the best expected conformers), or when conformers
 428 were generated by short MD trajectories, either using 100 or
 429 1,000 conformers (**Figure S4**). Strikingly, when we used the
 430 best conformers based on $C\alpha$ - or Int-RMSD with respect to the
 431 complex structure, the docking results were slightly worse than
 432 those of unbound docking, as can be seen in **Figure 4A** (the
 433 results did not significantly change when selecting only those
 434 cases in which the best conformer had significantly better $C\alpha$ -
 435 or Int-RMSD than that of the unbound structure). This can be
 436 due to the fact that either MODELER minimization or a short
 437 MD trajectory cannot generally sample too far from the
 438 unbound structure, and therefore cannot reach the vicinity of
 439 the bound state in most of the cases. However, when using the
 440 conformers that would give the best binding energy or the
 441 smallest number of clashes when in the native orientation, the
 442 docking results significantly improved with respect to those of
 443 the unbound structures, as can be seen in **Figure 4A**. Again, this
 444 did not correspond to an improvement in geometrical terms.
 445 Indeed, in 99% of the cases in which the best-energy conformer
 446 improved the docking predictions, such conformer did not have
 447 significantly better Int-RMSD from the complex structure than
 448 the unbound conformation. For comparison, we show the
 449 success rates that we would obtain when using the bound
 450 structures, which establishes the upper limit for the expected
 451 docking success with this approach. The success rates of the
 452 selected conformers based on binding energy are more than

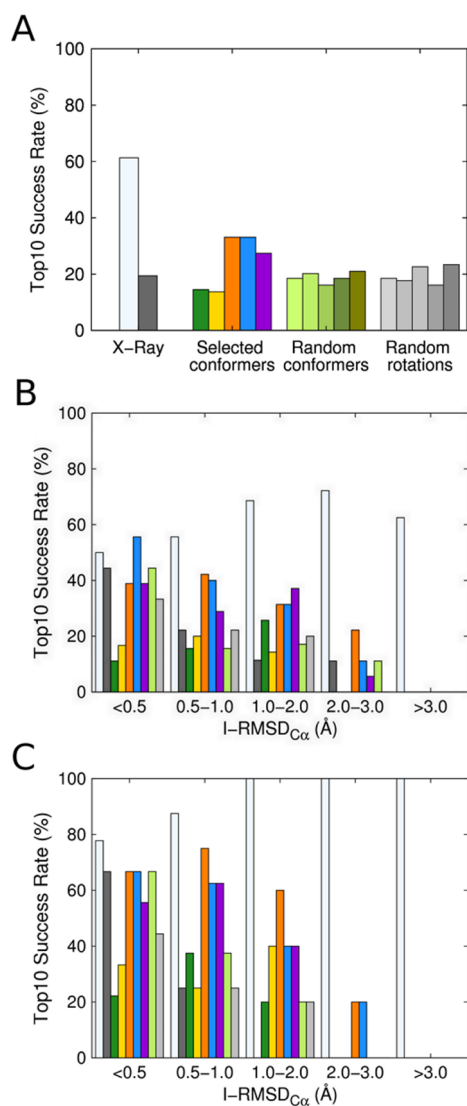


Figure 4. Docking performance for selected conformers. (A) Docking success rates for the top 10 predicted models on the protein–protein docking benchmark when using selected conformers according to specific criteria: $C\alpha$ -RMSD (green), Int-RMSD (yellow), binding energy toward the bound partner (orange), binding energy toward the unbound partner (blue), number of clashes with respect to the bound partner (magenta). For comparison, the docking success rates for bound (white) and unbound (dark gray) X-ray structures are also shown. To show the significance, docking rates for five random conformers pairs (green gradations) and five random initial rotations of the unbound docking partners (gray gradations) are also shown. (B) Docking success rates according to the conformational variability between the unbound and bound structures for selected conformers (same color code as above). For comparison, docking success rates for the bound and unbound X-ray structures, as well as for one random pair of conformers (light green) and one random initial rotation of the unbound docking partners (light gray) are also shown. (C) Docking success rates according to unbound–bound conformational variability on the 28 cases of the benchmark with reported high affinity ($\Delta G < -12.0$ kcal/mol) when using selected conformers, as well as the bound and unbound X-ray structures, one random pair of conformers and one random initial rotation of the unbound docking partners (same color code as above).

better docking predictions than the unbound structures. 456 However, in a realistic scenario, it would be impossible to 457 accurately identify these optimal conformers from the unbound 458 ensemble. The success rates obtained in this section can be 459 considered as a rough estimation of the potential predictive 460 rates that could be obtained if all ensemble conformers were 461 used in a docking strategy. One could hypothesize that if these 462 conformers are able to find docking orientations with good 463 scoring, such orientations would automatically appear well- 464 ranked in a general docking pool, even if they include docking 465 poses obtained with other conformers. Preliminary tests show 466 that merging the results of 100 docking runs with one 467 conformer from the receptor protein and another from the 468 ligand protein, each time a different one, would provide similar 469 success rates than the ones obtained here when using the best- 470 energy (with the unbound partner) conformers (data not 471 shown). There could be other strategies that can be devised for 472 using all unbound conformers in docking. However, the 473 systematic evaluation of these different approaches in a practical 474 docking procedure is beyond the scope of this work. The 475 findings here show some potentiality for future developments 476 in ensemble protein–protein docking, but the practical 477 problem is still unsolved. 478

In order to provide a statistical significance for these results, 479 we randomly selected five conformers from the conformational 480 ensemble. The results for each random conformer were similar 481 (within experimental error) to those of the unbound structure 482 (Figure 4A) and show that the conformers selected according 483 to the optimal binding energy improved significantly the 484 docking results with respect to the randomly chosen con- 485 formers. An alternative possible explanation for the docking 486 improvement when using the ensemble conformers might be 487 related to the limited discrete sampling in FTDock derived 488 from the fix number of ligand rotations (which makes coarser 489 surface sampling for large proteins) and the grid resolution of 490 0.7 Å (which introduces inaccuracies in the atomic 491 coordinates). This creates a stochastic dependence of the 492 FTDock docking algorithm on the initial rotation of the 493 interacting subunits, given that each initial rotation of the 494 interacting proteins could be mapped on different cells of the 495 3D grids. This is a limitation of any FFT-based algorithm, and it 496 was already shown that performing parallel docking runs using 497 several initial rotations provided more consistent docking 498 results than using just a single one.¹⁴ To evaluate the possibility 499 that the extensive sampling in the atomic positions provided by 500 the use of unspecific conformers prior to docking could 501 compensate the suboptimal grid-based sampling of FTDock, we 502 performed five different docking runs with random initial 503 rotations for the unbound receptor and ligand proteins. The 504 results from the individual random rotations were similar, 505 within experimental error, to the unbound docking results 506 (Figure 4A). 507

These results suggest that the selected conformers according 508 to specific criteria (i.e., optimal binding energy, number of 509 clashes) were more beneficial for docking than just a random 510 selection of conformers or initial rotations. Overall, this clearly 511 shows that conformational heterogeneity in the interacting 512 subunits can improve the binding capabilities of the unbound 513 X-ray structures. 514

A Simple Description of Conformational Heterogeneity Is Particularly Beneficial for Low- and Medium-Flexible Cases. We have analyzed whether the docking 515 improvement when using ensembles depends on the conforma- 516 517 518

453 half of the maximum expected success rates when using the 454 bound structures. It is important to mention that this approach 455 only proves the existence of some conformers that can provide

Table 1. Docking Performance of Conformers Selected from MODELLER Ensembles^a

PDB	bound	unbound	C α -RMSD	Int-RMSD	bound BE	unbound BE	clashes
Rigid (I-RMSD _{Cα} < 0.5 Å) (18 Cases)							
1AVX	2	102		33	40	1	231
1FSK	3	3	39	34	1	1	514
1GHQ	7455			6528		1878	
1IQD	1	8	64	3	6	6	3
1KLU	18	1246	6002	4468	2587	6498	1647
1KTZ	48	3725	6333				309
1NCA	14	7	1269		1332	7	1
1NSN	405	500	254	5587	33	33	1085
1PPE	28	6	12	2	5	1	4
1R0R	1	3	258	230	9	17	37
1SBB	161	298	73				
1WEJ	1	274	5	456	64	2	9
2JEL	1	42	16	25	12	2	1
2MTA	2	78	61	187	48	3	554
2PCC	12	6	91	12	6	4	11
2SIC	1	8	3378	1	2	249	1
2SNI	1	3	1	16	1	1	1
2UUY	69	4472	4801	64	159	11	1997
Low-Flexible (I-RMSD _{Cα} 0.5–1.0 Å) (45 cases)							
1AHW	1043	4049	6796	838	431	836	2974
1AY7	1	24	130	118	4	2	7
1AZS	1	30			6	6	
1BJ1	9				18	9	25
1BUH	71	66	209	426	36	24	119
1BVN	1	2	2	1	1	1	687
1DQJ	216	604	261	3363	75	25	223
1E96	113	1	59	168	73	5	130
1EAW	8	622	297	86	42	25	1
1EFN	6	166	197	1684	203	97	172
1EWY	4	8	200	5	10	10	1
1F34	1	139	174	226	52	280	2
1F51	2	7	13	375	1505	130	8
1FQJ	14	309	396	482	218	438	101
1GCQ	274	1091	574	1540	5	5	364
1GLA	61	50		12	6	21	131
1GPW	1	1	1	1	1	1	1
1HE1	1	3958	102	4506	2425	523	2629
1HE8	138	2917	2612	1503	277	242	3437
1IJK	16	1309	69	61	493	487	388
1J2J	46	19	303	18	2	3	5
1JPS	709	481		2135	1	2	
1K4C			3036	3369	2275		2379
1K74	150	14	172	82	1	1	24
1KAC	4737	1286	3545	990	107	19	917
1KXQ	1	250	8	4	4	1	1
1MAH	1	19	2	4	4	1	1
1MLC	2	37	50	10	1	97	144
1N8O	3	53			5		90
1QA9	3253	7378	5902	6152	1546	37	7973
1QFW	81	239	234		26	21	72
1RLB	1319	4094		7917			
1S1Q	147	1211	2994	541	164	175	87
1T6B	3	56	802	1464	2	11	3
1TMQ	1	1	27	4	54		4
1UDI	1	1	2	47	1	1	420
1YVB	1	19	1	2	3	21	7
1Z0K	2	8	523	57	42	11	44
1ZHI	5	3	7450		196	5	5
2AJF	5	1788		311	562	2268	2122
2B42	1	1	2	37	1	2	21

Table 1. continued

PDB	bound	unbound	C α -RMSD	Int-RMSD	bound BE	unbound BE	clashes
Low-Flexible (I-RMSD _{Cα} 0.5–1.0 Å) (45 cases)							
2BTF	1	33	120	26	60	9	250
2OOB	588	112	131	217	106	547	432
2VIS	64						
7CEI	1	19	11	1	1	1	20
Medium-Flexible (I-RMSD _{Cα} 1.0–2.0 Å) (35 Cases)							
1A2K	36	114	5641	284			782
1AK4	2420	2040	3983	3619		2721	1055
1AKJ	89	656	345	261	204	162	1168
1B6C	1	3	6	11	1	1	21
1BGX	1						
1BVK	7	18	4	146	87	85	2
1D6R	1050	2128	227	888	669	785	102
1DFJ	6	557	2	1	1	1	4
1E6E	1	3	2	1	1	8	1
1E6J		33	34	3	1	2	5
1EZU	1	2048	3633		1449	1547	102
1FC2	127		233	326	1256	683	171
1GP2	1			842	85		87
1GRN	2	858	184	1184	450	23	2909
1HIA	99	40	415	42	23	166	7
1I4D	1			642		44	132
1I9R	15	846	568	212		99	
1KSD	1	360	85		2	610	
1KXP	1	16	14	1	1	1	1
1ML0	1	173	80	140	1	1	9
1NW9	1	9	181	36	43	39	181
1OPH	59	14		469			2584
1VFB	37	59	86	59	128	31	95
1WQ1	4	2448	5	1077	16	6	6
1XD3	1	1	3	13	2	1	1
1XQS	1	14	55	628	1	8564	7
1Z5Y	1	16	320		4	39	17
2CFH	1	1904	202	1394	4066	43	5
2FD6	68	31				81	1
2H7V	1		734		1091		
2HLE	1	13	1	1	2	1	3
2HQS	1	30	2	30	146	146	129
2I25	1	40	443	1520	15	948	3599
2O8V	1	60	5	186	220	1	
2QFW	1		19			7	73
Flexible (I-RMSD _{Cα} 2.0–3.0 Å) (18 Cases)							
1ACB	1	361	144	668	6	4	15
1BKD	2	522	157	1050	99	114	646
1CGI	1	19	98	13	1	12	5
1DE4	1			366			
1E4K	104	1215	722	148	200	4249	74
1EER	3	1821	91	21	81	37	675
1I2M	1		683	632	50	149	247
1IB1	34		2116	7028	255	2775	1626
1IBR	1						
1KKL	88	49	271	176	1	2	289
1M10	1	81	5742	574		21	2873
1N2C	1					16	
1PXV	1	2073	100	429	673	1498	2375
2C0L	83	3958	1024	1589		5105	3834
2HMI	2						
2HRK	49	16	23	47	83	83	241
2NZ8	1	10	5509	247	2	168	5848
2OT3	1	5	212	14	91		131

Table 1. continued

PDB	bound	unbound	$C\alpha$ -RMSD	Int-RMSD	bound BE	unbound BE	clashes
Highly Flexible (I-RMSD $_{C\alpha}$ > 3.0 Å) (8 Cases)							
1ATN	7	2568				665	
1FAK	41	5327			43	41	
1FQJ	6	3865	4315	7901	927		4833
1H1V	537						
1IRA	1						
1JMO	1	5325		5398	2969	5510	5547
1R8S	1					4043	
1Y64	1420					1329	

^aFor each case, the best rank of any near-native docking solution is shown, when docking the bound and unbound structures of the interacting proteins, or the best conformers selected from the MODELER ensembles according to the different criteria, based on the native orientation, as described in the main text. In bold are shown the high-affinity cases.

tional rearrangement of the interacting proteins upon binding (see Methods). The largest docking improvement when using the selected conformers is observed in the low- and medium-flexible cases, i.e. those with I-RMSD $_{C\alpha}$ between 0.5 and 2.0 Å (Figure 4B). The ensemble success rates are particularly good in the low-flexible cases, for which they reach predictive docking values similar to the optimal ones when using the bound structures. This could be related to the limited sampling used here, which did not explore too far from the unbound (1.2 Å of Int-RMSD as average) and therefore they can only deeply explore the vicinity of the bound state in low-flexible or rigid cases. Indeed, in the rigid cases (I-RMSD $_{C\alpha}$ < 0.5 Å), the selected conformers yield similar results to the unbound structures. In these cases, unbound structures already produced optimal results, similar to the optimal success rates obtained when using the bound structures. In flexible or highly flexible cases (I-RMSD $_{C\alpha}$ > 2.0 Å), the docking results for the ensembles are as poor as those for the unbound structures, very far from the optimal success rates when using the bound structures. Using MD or more conformers does not significantly change the results (Figure S5).

We noted that the results of bound docking are not as good as one would expect, mostly due to the above-mentioned low-resolution FFT-based discrete searching algorithm. In this method, proteins are represented in 3D grids with 0.7 Å of grid cell size, and thus the exact atomic positions of the interacting proteins are not explicitly considered during the simulations. Rotations of the ligand protein are also discretely sampled, which makes it unlikely to find the exact native orientation. This would be particularly critical in low-affinity cases, in which the small number of interactions would make them less tolerant to small errors in the atomic positions. To minimize the impact of this technical limitation in our evaluation, we have performed the same analysis as above but focusing only on the 28 cases of the benchmark that have been experimentally defined as high-affinity (ΔG < -12.0 kcal/mol), for which the results of bound docking are close to optimal (Figure 4C). Under these conditions, we can observe even more clearly that the selected conformers largely improved the docking success rates in the low-flexible cases. This analysis helps to explain the observed general improvement in docking when using the optimal conformers and aims to be useful for future development of a practical docking protocol. Given that it would be very difficult to identify *a priori* which cases can be more benefited from this approach, any future docking protocol using this strategy should be of general applicability to all cases.

DISCUSSION

Conformers Providing Better Binding Energy in the Native Orientation Are More Likely To Improve Docking. We have shown that a set of discrete conformers representing the conformational heterogeneity of the unbound structure yielded better docking results than the unbound structures alone. It would be important to analyze the reasons for the success of such conformers. Surprisingly, the conformers that were structurally more similar to the reference structures did not yield better docking results than the unbound structures. More interestingly, selected conformers with the best binding energy in the native orientation yielded better docking results than the unbound structures. Thus, the capacity to provide favorable binding energy in the native orientation seems to be a major determinant for the success of docking, as opposed to the criterion of structural similarity to the native conformation. This might be due to the fact that in the majority of our cases, ensembles are not exploring the conformational space close to the bound state, because sampling is limited to a region in the vicinity of the unbound.

Figure 5A shows, for each case, the best ranked near-native solution obtained when docking the conformers that had the best native-oriented binding energy with the bound partner (i.e., best near-native rank in ordinates; average native-oriented energy of best pair of conformers in abscissas). As we can see in Figure 5A, 90% of the successful cases (i.e., near-native solution ranked within top 10) have an average conformer binding energy < -20.0 au in the native orientation. Actually, 71% of the docking cases with conformers with binding energy in the native orientation < -40.0 au were successful. This confirms that the existence of conformers with good optimal energy in the native orientation is determining the success of docking. Figure 5A highlights the cases that significantly improved, i.e. which had a near-native ranked ≤ 10 when using the energy-based selected conformers but not when using the unbound structures. In many of these cases, the unbound structures in the native orientation had binding energy < -20.0 au (Figure 5B) but were not successful in unbound docking. In these cases, a minimal amount of conformational sampling seems to be sufficient to generate conformers that significantly improve the docking results.

Ensembles in Docking: Does Size Really Matter? For a practical use in docking, the conformational ensembles should provide a reasonable coverage of the conformational space, using a minimal number of conformers. We have shown here that the selected conformers (based on the reference complex structure) from the 1,000-member ensembles generated by 611

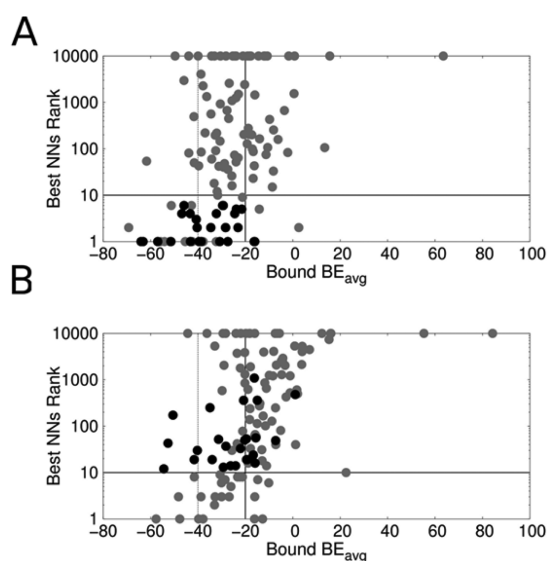


Figure 5. Docking performance dependence on energetic complementarity of the docking partners. Best rank of any near-native docking solution vs average native-oriented pyDock binding energy (au) toward the bound partner calculated for (A) best pair of conformers according to binding energy toward the bound state and (B) unbound X-ray structures. Highlighted in black are the cases that largely improve docking performance (from near-native rank >10 to rank ≤ 10) using the energy-based selected conformers.

612 MODELER or MD yielded similar results to those selected
613 from the 100-member ensembles (Figure S4). This suggests
614 that the “extra” 900 conformers are exploring the same
615 conformational region and that the initial ensembles of 100
616 conformers already achieved convergence and provided
617 reasonable sampling, at least at the conditions of our
618 experiment. Perhaps the resolution of the docking or the
619 energy-based scoring is not sufficient to appreciate subtle
620 changes in the conformational ensembles, so adding more
621 models, without changing the conditions of the simulation, is
622 not going to help. This is exactly what happens in the more
623 rigid cases, in which a larger conformational ensemble does not
624 seem to help to find better conformers to improve the docking
625 results. However, we can observe a small improvement in the
626 flexible cases when using the larger ensembles (Figure S5).
627 Perhaps, in addition to larger ensembles, higher conformational
628 variability would be needed in order to see further improve-
629 ment in the flexible cases. In this sense, we have performed
630 longer MD simulations (100 ns), at different temperatures (300
631 and 340 K), on a random selection of 11 cases with no missing
632 long loops (comprising all ranges of flexibility values). The
633 1,000-member ensembles from these extended MD simulations
634 showed larger conformational variability as compared to the
635 shorter simulations. However, these larger ensembles did not
636 increase the number of cases with conformers significantly
637 more similar to the bound structure, neither provided better
638 docking success rates (S1 Table). Given the known
639 convergence issues in MD,⁶³ it seems that more exhaustive
640 sampling of the unbound conformational space is needed for
641 most of the cases. This could be achieved by much longer MD
642 trajectories, multiple MD runs in parallel, or enhanced sampling
643 methods like metadynamics,⁶⁴ replica-exchange,⁶⁵ or MD with
644 excited normal modes.⁶⁶ Future work on ensemble docking
645 would need to explore the use of these enhanced ensembles.

Binding Mechanism: What Can We Learn from 646
Docking? The different possible mechanisms that have been 647
proposed for protein–protein association could be described by 648
existing computational approaches. In this context, we can 649
consider several possible scenarios. For protein complexes 650
following a rigid association (similar to “lock-and-key” 651
mechanism), the use of rigid-body docking with the unbound 652
subunits could be a suitable approach to describe the binding 653
process and obtain good predictive models. Indeed, this seems 654
to be the case for complexes with small conformational changes 655
between the unbound and bound states ($I\text{-RMSD}_{C\alpha} < 0.5 \text{ \AA}$), 656
in which unbound docking already gives similar success rates as 657
bound docking (Figures 4B and 4C). In these rigid cases, the 658
optimal conformers from the unbound ensembles also yielded 659
similarly good docking rates as those obtained with the 660
unbound and bound structures. Indeed, Figure 6 shows one 661 66

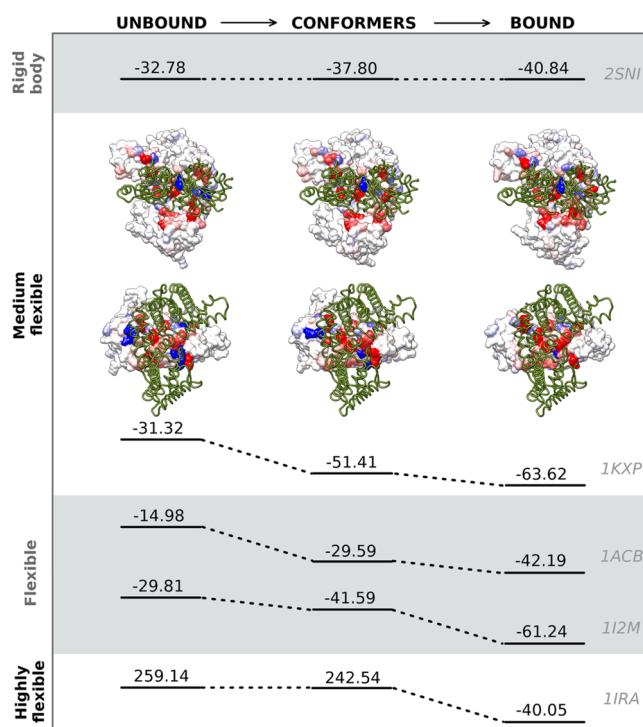


Figure 6. Average pyDock binding energy (au) of the unbound, best conformer according to native-oriented bound energy and bound conformations, in the native orientation, with the bound structure. A few examples with different degrees of unbound-to-bound conformational changes are shown. Similar binding energies for the unbound, conformer and bound structures suggest a lock-and-key binding mechanism (as in 2SNI). An average binding energy for conformers better than that of unbound structures and similar to that of bound structures suggests a conformational selection model (as in 1KXP, 1ACB). Conformer binding energy similar to that of the unbound conformation and worse than that of the bound structure could be compatible with conformational selection (1I2M; see main text) or induced fit mechanisms (1IRA).

example of rigid-body docking (2SNI) in which the unbound 662
proteins in the native orientation showed good average binding 663
energy toward the bound partner (-32.8 au), not far from that 664
of the bound structures (-40.8 au). Consistently, the average 665
binding energy of the best conformers were similar to that of 666
the unbound or bound pairs (-37.8 au). However, when 667
conformers were selected by criteria of structural similarity to 668
bound state, docking success rates were much worse than 669

Table 2. Docking Performance of Conformers Selected from NMA-Based Ensembles

PDB	bound	unbound	MM (100 conf)	MM (1,000 conf)	NMA (100 conf) * MM (1 conf)	NMA (100 conf) * MM (10 conf)	NMA (1,000 conf) * MM (1 conf)
1ACB	1	361	4 ^d	34 ^d	46 ^c	3 ^d	1 ^d
1ATN	7	2568	665 ^d		292 ^c	3245 ^a	1788 ^a
1EER	3	1821	21 ^b	13 ^c	17 ^d	3 ^c	3 ^b
1I2M	1		50 ^c	13 ^c	23 ^c	1 ^{c,d}	1 ^d
1IBR	1			1108 ^c	87 ^a	146 ^e	88 ^a
1PXV	1	2073	100 ^a	822 ^c	168 ^d	168 ^d	232 ^d

^a α global RMSD. ^bFull-atom interface RMSD. ^cNative-oriented binding energy with bound partner. ^dNative-oriented binding energy with unbound partner. ^eNumber of clashes with bound partner in the native orientation.

670 unbound or bound docking, because in these cases conformational heterogeneity is more likely to produce conformers that are further from the bound state than the unbound one (given that the unbound was already close to the bound state). Indeed, in none of these cases there were a single conformer that was significantly closer (in terms of Int-RMSD) to the bound state than the unbound structure.

677 On the other side, we know that in complexes involving flexible association, rigid-body docking with the unbound structures is not going to produce correct models. For such cases, different binding mechanisms have been proposed, such as conformational selection or induced fit. For cases following the conformational selection mechanism, the hypothesis is that the unbound proteins naturally sample a variety of conformational states, a subset of which are suitable to bind the other protein. Therefore, for these cases the use of precomputed unbound ensembles describing the conformational variability of the free proteins in solution should generate conformers that would improve the rigid-body docking predictions with respect to those with the unbound structures. Indeed, this is the case for the complexes undergoing unbound to bound transitions between 0.5 and 1.0 Å I-RMSD_{Ca}. In these cases, selected conformers from the unbound ensembles yielded much better docking predictions than the unbound structures, virtually achieving the success of bound docking (Figure 4B). For cases undergoing unbound-to-bound transition between 1.0 and 2.0 Å I-RMSD_{Ca} the use of unbound ensembles also improved the predictions with respect to the unbound docking results, although to a lesser extent (Figure 4B). Figure 6 shows one of these cases, 1KXP, in which the binding energy of the selected pair of conformers in the native orientation (−51.4 au) is better than that of the unbound structures (−31.3 au) and similar to that of the bound structures (−63.6 au). Some residues in the best pair of conformers show better energy contribution than in the unbound state, which explains why this specific pair of conformers improves docking results. In these cases, the existence of a subpopulation of “active” conformers, i.e. with good binding capabilities toward the bound partner, would be consistent with a conformational selection mechanism. The fact that these conformers with improved binding capabilities are not geometrically closer to the bound state seems counter-intuitive. However, recent views of binding mechanism suggest that active conformers that are selected by the partner (initial encounters) do not necessarily need to be in the bound state, as they can adjust their conformations during the association process.³⁵ Our docking poses are likely to represent these initial encounters between the most populated conformational states of the interacting proteins and would be compatible with this extended conformational selection view.³⁵ However, in other cases the limited conformational sampling used here might not

670 be sufficient to explore all conformational states available in solution, and therefore the specific binding mechanism cannot be easily identified.

673 On the other extreme, in cases following an “induced-fit” mechanism the bound complexes would only be obtained after rearrangement of the interfaces when interacting proteins are approaching to each other, in which case the use of precomputed conformational ensembles in docking (even if generated by exhaustive sampling) would not produce favorable encounters around the native complex structure. This seems the case for complexes undergoing unbound to bound transitions above 3.0 Å I-RMSD_{Ca}. In all these cases, rigid-body docking, either with unbound structures or with selected conformers, fails to reproduce the experimental complex structure. Figure 6 shows one of these highly flexible cases, 1IRA, in which the binding energy of the selected pair of conformers is similar to that of the unbound structures and much worse than that of the bound conformation. For these complexes, the use of precomputed unbound ensembles does not seem to be advantageous, and they would probably need to include flexibility during the docking search, mimicking the induced fit mechanism. However, in the flexible category (i.e., unbound to bound transitions between 2.0 and 3.0 Å I-RMSD_{Ca}), there are cases like 1ACB, which seem to follow the (extended) conformational selection mechanism, since the use of conformers helps to improve the docking results, and the conformers show better energy than the unbound structures (Figure 6). Again, there might be other complexes under this category that could still follow the conformational selection mechanism, but for which our conformational search is perhaps not sufficient to sample the productive conformations that may exist in solution. This seems to be the case of 1I2M, in which the ensembles based on MODELER did not produce any pair of conformers with sufficiently good binding energy in the native orientation (Figure 6), but the use of extended sampling based on NMA was able to improve the docking rates (see later).

677 Obviously, the use of docking calculations to learn about the binding mechanism has additional limitations. The time scale of transitions between inactive and active conformers can play an important role in controlling the binding mechanism.⁶⁷ In the present work, we can only assume that our ensembles are formed by the most populated conformers in solution, so the existence of active conformers that can be preferentially selected by the bound partner would be compatible (but not exclusively) with a mainly conformational selection mechanism. However, in a situation in which the active conformers are not highly populated, as those that would need extended sampling to be identified, we could not define the type of mechanism unless transition rates between conformers are considered.

770 **Future Perspectives: Improving Sampling with Normal-Mode Analysis for Flexible Cases.** We have shown
771 here that cases with large conformational changes after binding
772 (I-RMSD_{C α} > 2 Å) do not generally benefit from the use of
773 conformers from unbound ensembles generated by MODELER
774 or short MD simulations. These complexes could follow the
775 induced fit binding mechanism, in which the use of
776 precomputed unbound ensembles would not be appropriate
777 to describe association. However, we should not disregard that
778 some of these complexes could still follow a conformational
779 selection mechanism, but for some reason a dramatically larger
780 conformational sampling would be needed to find suitable
781 conformers. One way to extend conformational sampling is by
782 using Normal Mode Analysis (NMA). When generating 100
783 conformers for this group of cases (strong and flexible I-
784 RMSD_{C α} > 2.0 Å) with an *ad-hoc* Monte Carlo sampling
785 method based on C α NMA and full-atom rebuilding with
786 MODELER (Figure S6; see Methods), the results were not
787 better than those obtained with the conformers directly
788 generated by MODELER (Tables 2 and S2). However, when
789 generating 1,000 conformers based on NMA (either formed by
790 1,000 NMA-based conformers rebuilt with MODELER, or by
791 100 NMA-based conformers with 10 MODELER models for
792 each of them), the success rates largely improved with respect
793 to those obtained when generating conformers only with
794 MODELER (either 100 or 1,000 conformers). It is interesting
795 to analyze the flexible case 112M, in which docking failed when
796 using the unbound structure or the best conformers from either
797 MODELER or MD ensembles, but yielded successful results
798 with the 1,000-member NMA-based ensembles. This shows
799 that new sampling approaches based on NMA could produce
800 the type of enhanced sampling needed for the most flexible
801 cases that follow a conformational selection mechanism. Our
802 findings could help to develop future strategies to integrate
803 NMA-sampling in a practical docking protocol, but this would
804 need extensive evaluation on the entire benchmark (including
805 cases in which the conformational difference between bound
806 and unbound structures is small) and algorithmic optimization,
807 which is beyond the scope of current work.

809 ■ CONCLUSIONS

810 We present here the most complete systematic study so far
811 about the potential capabilities of using precomputed unbound
812 ensembles in docking. The results show that considering
813 conformational heterogeneity in the unbound state of the
814 interacting proteins can improve their binding capabilities in
815 cases of moderate unbound-to-bound mobility. In these cases,
816 the existence of conformers with better binding energy in the
817 native orientation is associated with a significant improvement
818 in the docking predictions. It seems that protein plasticity
819 increases the chances of finding conformations with better
820 binding energy capabilities, not necessarily related to similar-to-
821 bound geometries, which is compatible with the extended
822 conformational selection mechanism. Other moderately flexible
823 cases have conformers that look promising from a binding
824 energy perspective but do not provide good docking
825 predictions. These cases could also follow a conformational
826 selection mechanism, but they would need extensive sampling
827 to find suitable conformers for binding. The most flexible cases
828 would show larger induced fit effects and therefore would not
829 be well described by ensemble binding. In a realistic scenario,
830 optimal conformers would not be easy to identify *a priori*, and,
831 as a consequence, new ways of efficiently including all

conformers in a docking protocol should be devised. This
work helps to set guidelines for future strategies in practical
docking predictions based on unbound ensembles generated by
molecular mechanics minimization.

■ ASSOCIATED CONTENT

Supporting Information

The Supporting Information is available free of charge on the
ACS Publications website at DOI: 10.1021/acs.jctc.6b00204.

Figure S1: Distribution of conformers according to
different quality criteria in the 100-member ensembles.
Figure S2: Representative conformational ensembles
generated by 10 ns MD simulations. Figure S3:
Distribution of conformers according to different quality
criteria in the 1,000-member ensembles. Figure S4:
Docking performance for the best conformers of
different ensembles. Figure S5: Docking performance
for the different ensembles according to unbound-to-
bound variability. Figure S6: Representative conforma-
tional ensembles generated by NMA-based sampling.
Table S1: Docking performance (best rank of any near-
native solution) with conformers selected from extended
MD ensembles. Table S2: Docking performance of
conformers selected from NMA-based ensembles (PDF)

■ AUTHOR INFORMATION

Corresponding Author

*E-mail: juanf@bsc.es.

Author Contributions

The manuscript was written through contributions of all
authors. All authors have given approval to the final version of
the manuscript.

Funding

This work was supported by grant BIO2013-48213-R from the
Spanish Ministry of Economy and Competitiveness. R.A. was
partially supported by NIH (R01 GM071872) and is a founder
and shareholder in Molsoft, LLC.

Notes

The authors declare no competing financial interest.

■ ACKNOWLEDGMENTS

We thank Dr. Iain Moal for the extended molecular dynamics
trajectories.

■ ABBREVIATIONS

MD, molecular dynamics; NMA, normal modes analysis;
eNMA, enhanced normal modes analysis; RMSD, root-mean-
square deviations; CAPRI, Critical Assessment of PRediction of
Interactions; NMR, nuclear magnetic resonance; RDC,
Residual Dipolar Coupling; MM, modeling minimization; BE,
binding energy; FFT, Fast Fourier Transform

■ REFERENCES

- (1) Alberts, B. The cell as a collection of protein machines: preparing the next generation of molecular biologists. *Cell* **1998**, *92*, 291–4.
- (2) Rual, J. F.; Venkatesan, K.; Hao, T.; Hirozane-Kishikawa, T.; Dricot, A.; Li, N.; Berriz, G. F.; Gibbons, F. D.; Dreze, M.; Ayivi-Guedehoussou, N.; Klitgord, N.; Simon, C.; Boxem, M.; Milstein, S.; Rosenberg, J.; Goldberg, D. S.; Zhang, L. V.; Wong, S. L.; Franklin, G.; Li, S.; Albalá, J. S.; Lim, J.; Fraughton, C.; Llamasas, E.; Cevik, S.; Bex, C.; Lamesch, P.; Sikorski, R. S.; Vandenhaute, J.; Zoghbi, H. Y.; Smolyar, A.; Bosak, S.; Sequerra, R.; Doucette-Stamm, L.; Cusick, M.

- 889 E.; Hill, D. E.; Roth, F. P.; Vidal, M. Towards a proteome-scale map of
890 the human protein-protein interaction network. *Nature* **2005**, *437*,
891 1173–8.
- 892 (3) Stelzl, U.; Worm, U.; Lalowski, M.; Haenig, C.; Brembeck, F. H.;
893 Goehler, H.; Stroedicke, M.; Zenkner, M.; Schoenherr, A.; Koeppen,
894 S.; Timm, J.; Mintzlauff, S.; Abraham, C.; Bock, N.; Kietzmann, S.;
895 Goedde, A.; Toksoz, E.; Droege, A.; Krobitsch, S.; Korn, B.;
896 Birchmeier, W.; Lehrach, H.; Wanker, E. E. A human protein-protein
897 interaction network: a resource for annotating the proteome. *Cell*
898 **2005**, *122*, 957–68.
- 899 (4) Mosca, R.; Ceol, A.; Aloy, P. Interactome3D: adding structural
900 details to protein networks. *Nat. Methods* **2013**, *10*, 47–53.
- 901 (5) Szilagy, A.; Zhang, Y. Template-based structure modeling of
902 protein-protein interactions. *Curr. Opin. Struct. Biol.* **2014**, *24*, 10–23.
- 903 (6) Kundrotas, P. J.; Zhu, Z.; Janin, J.; Vakser, I. A. Templates are
904 available to model nearly all complexes of structurally characterized
905 proteins. *Proc. Natl. Acad. Sci. U. S. A.* **2012**, *109*, 9438–41.
- 906 (7) Kundrotas, P. J.; Vakser, I. A. Global and local structural similarity
907 in protein-protein complexes: implications for template-based docking.
908 *Proteins: Struct., Funct., Genet.* **2013**, *81*, 2137–42.
- 909 (8) Katchalski-Katzir, E.; Shariv, I.; Eisenstein, M.; Friesem, A. A.;
910 Afalo, C.; Vakser, I. A. Molecular surface recognition: determination
911 of geometric fit between proteins and their ligands by correlation
912 techniques. *Proc. Natl. Acad. Sci. U. S. A.* **1992**, *89*, 2195–9.
- 913 (9) Gabb, H. A.; Jackson, R. M.; Sternberg, M. J. Modelling protein
914 docking using shape complementarity, electrostatics and biochemical
915 information. *J. Mol. Biol.* **1997**, *272*, 106–20.
- 916 (10) Kozakov, D.; Brenke, R.; Comeau, S. R.; Vajda, S. PIPER: an
917 FFT-based protein docking program with pairwise potentials. *Proteins:*
918 *Struct., Funct., Genet.* **2006**, *65*, 392–406.
- 919 (11) Tovchigrechko, A.; Vakser, I. A. GRAMM-X public web server
920 for protein-protein docking. *Nucleic Acids Res.* **2006**, *34* (WebServer
921 issue), W310–W314.
- 922 (12) Chen, R.; Li, L.; Weng, Z. ZDOCK: an initial-stage protein-
923 docking algorithm. *Proteins: Struct., Funct., Genet.* **2003**, *52*, 80–7.
- 924 (13) Ritchie, D. W.; Kemp, G. J. Protein docking using spherical
925 polar Fourier correlations. *Proteins: Struct., Funct., Genet.* **2000**, *39*,
926 178–194.
- 927 (14) Garzon, J. I.; Lopez-Blanco, J. R.; Pons, C.; Kovacs, J.; Abagyan,
928 R.; Fernandez-Recio, J.; Chacon, P. FRODOCK: a new approach for
929 fast rotational protein-protein docking. *Bioinformatics* **2009**, *25*, 2544–
930 51.
- 931 (15) Schneidman-Duhovny, D.; Inbar, Y.; Nussinov, R.; Wolfson, H.
932 J. PatchDock and SymmDock: servers for rigid and symmetric
933 docking. *Nucleic Acids Res.* **2005**, *33* (Web Server issue), W363–
934 W367.
- 935 (16) Dominguez, C.; Boelens, R.; Bonvin, A. M. HADDOCK: a
936 protein-protein docking approach based on biochemical or biophysical
937 information. *J. Am. Chem. Soc.* **2003**, *125*, 1731–7.
- 938 (17) Lyskov, S.; Gray, J. J. The RosettaDock server for local protein-
939 protein docking. *Nucleic Acids Res.* **2008**, *36* (WebServer issue),
940 W233–W238.
- 941 (18) Fernandez-Recio, J.; Totrov, M.; Abagyan, R. Soft protein-
942 protein docking in internal coordinates. *Protein Sci.* **2002**, *11*, 280–91.
- 943 (19) Cheng, T. M.; Blundell, T. L.; Fernandez-Recio, J. pyDock:
944 electrostatics and desolvation for effective scoring of rigid-body
945 protein-protein docking. *Proteins: Struct., Funct., Genet.* **2007**, *68*, 503–
946 15.
- 947 (20) Pons, C.; Talavera, D.; de la Cruz, X.; Orozco, M.; Fernandez-
948 Recio, J. Scoring by intermolecular pairwise propensities of exposed
949 residues (SIPPER): a new efficient potential for protein-protein
950 docking. *J. Chem. Inf. Model.* **2011**, *51*, 370–7.
- 951 (21) Ravikant, D. V.; Elber, R. PIE-efficient filters and coarse grained
952 potentials for unbound protein-protein docking. *Proteins: Struct.,*
953 *Funct., Genet.* **2010**, *78*, 400–19.
- 954 (22) Lensink, M. F.; Wodak, S. J. Docking, scoring, and affinity
955 prediction in CAPRI. *Proteins: Struct., Funct., Genet.* **2013**, *81*, 2082–
956 95.
- (23) Pons, C.; Grosdidier, S.; Solernou, A.; Perez-Cano, L.; 957
Fernandez-Recio, J. Present and future challenges and limitations in 958
protein-protein docking. *Proteins: Struct., Funct., Genet.* **2010**, *78*, 95– 959
108. 960
- (24) Pallara, C.; Jimenez-Garcia, B.; Perez-Cano, L.; Romero-Durana, 961
M.; Solernou, A.; Grosdidier, S.; Pons, C.; Moal, I. H.; Fernandez- 962
Recio, J. Expanding the frontiers of protein-protein modeling: from 963
docking and scoring to binding affinity predictions and other 964
challenges. *Proteins: Struct., Funct., Genet.* **2013**, *81*, 2192–200. 965
- (25) Fernandez-Recio, J.; Totrov, M.; Abagyan, R. ICM-DISCO 966
docking by global energy optimization with fully flexible side-chains. 967
Proteins: Struct., Funct., Genet. **2003**, *52*, 113–7. 968
- (26) Mashiach, E.; Nussinov, R.; Wolfson, H. J. FiberDock: Flexible 969
induced-fit backbone refinement in molecular docking. *Proteins: Struct.,* 970
Funct., Genet. **2010**, *78*, 1503–19. 971
- (27) Zacharias, M. Protein-protein docking with a reduced protein 972
model accounting for side-chain flexibility. *Protein Sci.* **2003**, *12*, 1271– 973
82. 974
- (28) Zacharias, M. Rapid protein-ligand docking using soft modes 975
from molecular dynamics simulations to account for protein 976
deformability: binding of FK506 to FKBP. *Proteins: Struct., Funct.,* 977
Genet. **2004**, *54*, 759–67. 978
- (29) Moal, I. H.; Bates, P. A. SwarmDock and the use of normal 979
modes in protein-protein docking. *Int. J. Mol. Sci.* **2010**, *11*, 3623–48. 980
- (30) Straub, F. B.; Szabolcsi, G. O dinamiceszkij aspektah sztukturü 981
fermentov (On the dynamic aspects of protein structure). In *Molecular* 982
Biology, Problems and Perspectives; Braunstein, A. E., Ed.; Izdat. Nauka: 983
Moscow, 1964; pp 182–187. 984
- (31) Závodszy, P.; Abaturov, L. V.; Varshavsky, Y. M. Structure of 985
glyceraldehyde-3-phosphate dehydrogenase and its alteration by 986
coenzyme binding. *Acta Biochim. Biophys. Acad. Sci. Hung.* **1966**, *1*, 987
389–403. 988
- (32) Foote, J.; Milstein, C. Conformational isomerism and the 989
diversity of antibodies. *Proc. Natl. Acad. Sci. U. S. A.* **1994**, *91*, 10370– 990
4. 991
- (33) Tsai, C. J.; Ma, B.; Nussinov, R. Folding and binding cascades: 992
shifts in energy landscapes. *Proc. Natl. Acad. Sci. U. S. A.* **1999**, *96*, 993
9970–2. 994
- (34) Ma, B.; Kumar, S.; Tsai, C. J.; Nussinov, R. Folding funnels and 995
binding mechanisms. *Protein Eng., Des. Sel.* **1999**, *12*, 713–20. 996
- (35) Csermely, P.; Palotai, R.; Nussinov, R. Induced fit, conforma- 997
tional selection and independent dynamic segments: an extended view 998
of binding events. *Trends Biochem. Sci.* **2010**, *35* (10), 539–46. 999
- (36) Stein, A.; Rueda, M.; Panjkovich, A.; Orozco, M.; Aloy, P. A 1000
systematic study of the energetics involved in structural changes upon 1001
association and connectivity in protein interaction networks. *Structure* 1002
2011, *19*, 881–9. 1003
- (37) Boehr, D. D.; Nussinov, R.; Wright, P. E. The role of dynamic 1004
conformational ensembles in biomolecular recognition. *Nat. Chem.* 1005
Biol. **2009**, *5*, 789–96. 1006
- (38) Fraser, J. S.; Clarkson, M. W.; Degnan, S. C.; Erion, R.; Kern, 1007
D.; Alber, T. Hidden alternative structures of proline isomerase 1008
essential for catalysis. *Nature* **2009**, *462*, 669–73. 1009
- (39) Volkman, B. F.; Lipson, D.; Wemmer, D. E.; Kern, D. Two-state 1010
allosteric behavior in a single-domain signaling protein. *Science* **2001**, 1011
291, 2429–2433. 1012
- (40) Moal, I. H.; Bates, P. A. Kinetic rate constant prediction 1013
supports the conformational selection mechanism of protein binding. 1014
PLoS Comput. Biol. **2012**, *8*, e1002351. 1015
- (41) Bastard, K.; Thureau, A.; Lavery, R.; Prevost, C. Docking 1016
macromolecules with flexible segments. *J. Comput. Chem.* **2003**, *24*, 1017
1910–20. 1018
- (42) Bastard, K.; Prevost, C.; Zacharias, M. Accounting for loop 1019
flexibility during protein-protein docking. *Proteins: Struct., Funct.,* 1020
Genet. **2006**, *62*, 956–69. 1021
- (43) van Dijk, M.; van Dijk, A. D.; Hsu, V.; Boelens, R.; Bonvin, A. 1022
M. Information-driven protein-DNA docking using HADDOCK: it is 1023
a matter of flexibility. *Nucleic Acids Res.* **2006**, *34*, 3317–3325. 1024

- 1025 (44) Grunberg, R.; Leckner, J.; Nilges, M. Complementarity of
1026 structure ensembles in protein-protein binding. *Structure* **2004**, *12*,
1027 2125–36.
- 1028 (45) Smith, G. R.; Sternberg, M. J.; Bates, P. A. The relationship
1029 between the flexibility of proteins and their conformational states on
1030 forming protein-protein complexes with an application to protein-
1031 protein docking. *J. Mol. Biol.* **2005**, *347*, 1077–101.
- 1032 (46) Chaudhury, S.; Gray, J. J. Conformer selection and induced fit in
1033 flexible backbone protein-protein docking using computational and
1034 NMR ensembles. *J. Mol. Biol.* **2008**, *381*, 1068–87.
- 1035 (47) Pons, C.; Fenwick, R. B.; Esteban-Martín, S.; Salvatella, X.;
1036 Fernandez-Recio, J. Validated Conformational Ensembles Are Key for
1037 the Successful Prediction of Protein Complexes. *J. Chem. Theory*
1038 *Comput.* **2013**, *9*, 1830–1837.
- 1039 (48) Eswar, N.; Webb, B.; Marti-Renom, M. A.; Madhusudhan, M. S.;
1040 Eramian, D.; Shen, M. Y.; Pieper, U.; Sali, A. Comparative protein
1041 structure modeling using Modeller. *Curr. Protoc Bioinformatics*; 2006;
1042 Chapter 5, Unit 5.6.10.1002/0471250953.bi0506s15
- 1043 (49) Cheatham, T. E., 3rd; Cieplak, P.; Kollman, P. A. A modified
1044 version of the Cornell et al. force field with improved sugar pucker
1045 phases and helical repeat. *J. Biomol. Struct. Dyn.* **1999**, *16*, 845–862.
- 1046 (50) Case, D. A.; Cheatham, T. E., 3rd; Darden, T.; Gohlke, H.; Luo,
1047 R.; Merz, K. M., Jr.; Onufriev, A.; Simmerling, C.; Wang, B.; Woods, R.
1048 J. The Amber biomolecular simulation programs. *J. Comput. Chem.*
1049 **2005**, *26*, 1668–88.
- 1050 (51) Meyer, T.; D'Abramo, M.; Hospital, A.; Rueda, M.; Ferrer-
1051 Costa, C.; Perez, A.; Carrillo, O.; Camps, J.; Fenollosa, C.;
1052 Repchevsky, D.; Gelpi, J. L.; Orozco, M. MoDEL (Molecular
1053 Dynamics Extended Library): a database of atomistic molecular
1054 dynamics trajectories. *Structure* **2010**, *18*, 1399–409.
- 1055 (52) Wang, J.; Wang, W.; Kollman, P. A.; Case, D. A. Automatic
1056 atom type and bond type perception in molecular mechanical
1057 calculations. *J. Mol. Graphics Modell.* **2006**, *25*, 247–260.
- 1058 (53) Tirion, M. M. Large Amplitude Elastic Motions in Proteins from
1059 a Single-Parameter, Atomic Analysis. *Phys. Rev. Lett.* **1996**, *77*, 1905–
1060 1908.
- 1061 (54) Atilgan, A. R.; Durell, S. R.; Jernigan, R. L.; Demirel, M. C.;
1062 Keskin, O.; Bahar, I. Anisotropy of fluctuation dynamics of proteins
1063 with an elastic network model. *Biophys. J.* **2001**, *80*, 505–15.
- 1064 (55) Kovacs, J. A.; Chacon, P.; Abagyan, R. Predictions of protein
1065 flexibility: first-order measures. *Proteins: Struct., Funct., Genet.* **2004**, *56*,
1066 661–8.
- 1067 (56) Hinsen, K. Analysis of domain motions by approximate normal
1068 mode calculations. *Proteins: Struct., Funct., Genet.* **1998**, *33*, 417–429.
- 1069 (57) Rueda, M.; Chacon, P.; Orozco, M. Thorough validation of
1070 protein normal mode analysis: a comparative study with essential
1071 dynamics. *Structure* **2007**, *15*, 565–75.
- 1072 (58) Sali, A.; Blundell, T. L. Comparative protein modelling by
1073 satisfaction of spatial restraints. *J. Mol. Biol.* **1993**, *234*, 779–815.
- 1074 (59) Hwang, H.; Pierce, B.; Mintseris, J.; Janin, J.; Weng, Z. Protein-
1075 protein docking benchmark version 3.0. *Proteins: Struct., Funct., Genet.*
1076 **2008**, *73*, 705–9.
- 1077 (60) Abagyan, R.; Lee, W. H.; Raush, E.; Budagyan, L.; Totrov, M.;
1078 Sundstrom, M.; Marsden, B. D. Disseminating structural genomics
1079 data to the public: from a data dump to an animated story. *Trends*
1080 *Biochem. Sci.* **2006**, *31*, 76–8.
- 1081 (61) Garbuzynskiy, S. O.; Melnik, B. S.; Lobanov, M. Y.; Finkelstein,
1082 A. V.; Galzitskaya, O. V. Comparison of X-ray and NMR structures: is
1083 there a systematic difference in residue contacts between X-ray and
1084 NMR-resolved protein structures? *Proteins: Struct., Funct., Genet.* **2005**,
1085 *60*, 139–147.
- 1086 (62) Lindorff-Larsen, K.; Piana, S.; Palmo, K.; Maragakis, P.; Klepeis,
1087 J. L.; Dror, R. O.; Shaw, D. E. Improved side-chain torsion potentials
1088 for the Amber ff99SB protein force field. *Proteins: Struct., Funct., Genet.*
1089 **2010**, *78*, 1950–1958.
- 1090 (63) Lyman, E.; Zuckerman, D. M. On the structural convergence of
1091 biomolecular simulations by determination of the effective sample size.
1092 *J. Phys. Chem. B* **2007**, *111*, 12876–82.
- (64) Laio, A.; Parrinello, M. Escaping free-energy minima. *Proc. Natl.* 1093
Acad. Sci. U. S. A. **2002**, *99*, 12562–12566. 1094
- (65) Sugita, Y.; Okamoto, Y. Replica-exchange molecular dynamics 1095
method for protein folding. *Chem. Phys. Lett.* **1999**, *314*, 141–151. 1096
- (66) Costa, M. G. S.; Batista, P. R.; Bisch, P. M.; Perahia, D. 1097
Exploring free energy landscapes of large conformational changes: 1098
molecular dynamics with excited normal modes. *J. Chem. Theory* 1099
Comput. **2015**, *11*, 2755–2767. 1100
- (67) Zhou, H. X. From induced fit to conformational selection: a 1101
continuum of binding mechanism controlled by the timescale of 1102
conformational transitions. *Biophys. J.* **2010**, *98* (6), L15–7. 1103